AIP | Journal of Applied Physics

# Optical modeling of a-Si:H solar cells with rough interfaces: Effect of back contact and interface roughness

M. Zeman, R. A. C. M. M. van Swaaij, J. W. Metselaar, and R. E. I. Schropp

Citation: J. Appl. Phys. 88, 6436 (2000); doi: 10.1063/1.1324690
View online: http://dx.doi.org/10.1063/1.1324690
View Table of Contents: http://jap.aip.org/resource/1/JAPIAU/v88/i11
Published by the American Institute of Physics.

# Optical modeling of *a*-Si:H solar cells with rough interfaces: Effect of back contact and interface roughness

M. Zeman,[a] R. A. C. M. M. van Swaaij, and J. W. Metselaar
*Laboratory of Electronic Components, Technology and Materials, Delft University of Technology DIMES, P.O. Box 5053, 2600 GB Delft, The Netherlands*

R. E. I. Schropp
*Department of Atomic & Interface Physics, Utrecht University, Debye Institute, P.O. Box 80000, 3508 TA Utrecht, The Netherlands*

(Received 5 June 2000; accepted for publication 20 September 2000)

An approach to study the optical behavior of hydrogenated amorphous silicon solar cells with rough interfaces using computer modeling is presented. In this approach the descriptive haze parameters of a light scattering interface are related to the root mean square roughness of the interface. Using this approach we investigated the effect of front window contact roughness and back contact material on the optical properties of a single junction *a*-Si:H superstrate solar cell. The simulation results for *a*-Si:H solar cells with $SnO_2$:F as a front contact and ideal Ag, ZnO/Ag, and Al/Ag as a back contact are shown. For cells with an absorber layer thickness of 150–600 nm the simulations demonstrate that the gain in photogenerated current density due to the use of a textured superstrate is around 2.3 mA $cm^{-2}$ in comparison to solar cells with flat interfaces. The effect of the front and back contact roughness on the external quantum efficiency (QE) of the solar cell for different parts of the light spectrum was determined. The choice of the back contact strongly influences the QE and the absorption in the nonactive layers for the wavelengths above 650 nm. A practical Ag back contact can be successfully simulated by introducing a thin buffer layer between the *n*-type *a*-Si:H and Ag back contact, which has optical properties similar to Al, indicating that the actual reflection at the *n*-type *a*-Si:H/Ag interface is smaller than what is expected from the respective bulk optical parameters. In comparison to the practical Ag contact the QE of the cell can be strongly improved by using a ZnO layer at the Ag back contact or an *ideal* Ag contact. The photogenerated current densities for a solar cell with a 450 nm thick intrinsic *a*-Si:H layer with ZnO/Ag and ideal Ag are 16.7 and 17.3 mA $cm^{-2}$, respectively, compared to 14.4 mA $cm^{-2}$ for the practical Ag back contact. The effect of increasing the roughness of the contact interfaces was investigated for both superstrate and substrate types of solar cells. Increasing the roughness of the carrier electrode, i.e., the rough electrode on which the silicon cell structure is deposited, up to 35 nm leads to a strong increase in the photogenerated current density; for higher values of the interface roughness the photogenerated current density tends to saturate. © *2000 American Institute of Physics.* [S0021-8979(00)07724-0]

## I. INTRODUCTION

Light trapping has become a standard technique to increase absorption of the incident light in the active layers of hydrogenated amorphous silicon (*a*-Si:H) based solar cells. In highly efficient *a*-Si:H solar cells this technique is based mainly on the use of textured substrates and highly reflective back contacts. The idea of light absorption enhancement by employing a textured substrate, which introduces rough interfaces in the solar cell, is to take advantage of light scattering at a rough interface. Part of the light that reaches a rough interface will be scattered in various directions instead of propagating in the specular direction. In this way the average length of the light path in a layer is increased and the light absorption enhanced. Scattering at rough interfaces not only leads to enhancement of the absorption in the active intrinsic *a*-Si:H layer of the cell but also influences the absorption in all other layers. For an optimal optical design of *a*-Si:H solar cells it is important to know the light absorption profile in the whole solar cell. Since it is not easy to determine this profile experimentally,[1] computer modeling has proved to be a useful tool to study the absorption in *a*-Si:H solar cells. The use of modeling for optical design has, however, urged the development of optical models, which can accurately calculate the optical behavior of *a*-Si:H solar cells taking into account scattering at the rough interfaces.[2–10]

The numerical optical programs that take scattering into account require input data, which describe the scattering of light at a rough interface. The haze parameter, which is the ratio between the diffused part of the reflected (transmitted) light to the total reflected (transmitted) light, and the angular distribution of the diffuse light are of major importance. So far little is known about these descriptive scattering parameters of rough interfaces in *a*-Si:H solar cells and only a small amount of experimentally determined scattering data is available.[6,11–13] In addition, the general use of the available experimental data is limited, because they depend on the

[a]Author to whom correspondence should be addressed; electronic mail: m.zeman@its.tudelft.nl

 

morphology of a particular rough interface and on the optical properties of the two media that form the interface. Furthermore, in the above-mentioned experimental work no link between the scattering data and the roughness of the interface has been made.

In this article we investigate the optical behavior of *a*-Si:H solar cells as a function of interface roughness. Therefore we introduce a novel approach, in which we relate the required input haze parameters to the geometrical roughness of a rough interface. This relationship between the haze parameters and the interface roughness is important because the roughness parameters vary for the different interfaces in *a*-Si:H solar cells, as deposition of *a*-Si:H on a textured substrate smoothens the rough surface.[14]

This article is organized as follows. In Sec. II we describe the experimental details of preparation and characterization of the individual layers and complete solar cells that have been used in this work. For the simulations of the optical behavior of *a*-Si:H solar cells we use the GENPRO2 optical program.[4] After a short description of the GENPRO2 optical program in Sec. III, we present the relations between the diffuse part of the reflected and the transmitted light, and the interface roughness in Sec. IV. The interface roughness is characterized by the root mean square (rms) roughness $\sigma_r$, obtained from atomic force microscopy (AFM) data. We apply these relations to calculate the diffuse light at all rough interfaces in single junction *a*-Si:H solar cells. In Sec. V we check the validity of our approach first by simulating the external quantum efficiency (QE) and compare it with the measured QE for a series of four single junction *a*-Si:H solar cells with different thicknesses of the intrinsic layer. After demonstrating the validity of our approach by obtaining a good match between the measured and simulated (QE) data for all thicknesses using the same parameter set, we present simulation results, in which we vary the $\sigma_r$ of the interfaces. In particular, we investigate the effect of the front and back contact $\sigma_r$ on the absorption in all individual layers of a single junction *a*-Si:H solar cell. The effect of increasing the roughness of the contact interfaces is investigated for both the superstrate and substrate type cell. In addition, we also study the effect of back contact materials on the absorption profile in the solar cell.

## II. EXPERIMENT

### A. Optical properties of *a*-Si:H based layers

The GENPRO2 program requires as input optical constants (the refractive index and the extinction coefficient) of all individual layers, which form the simulated structure. We determined these quantities for each *a*-Si:H based layer that is used in our single junction *a*-Si:H solar cell. The *a*-Si:H layers were deposited on Corning glass substrate and measured by reflection and transmission spectroscopy, dual beam photoconductivity, and photothermal deflection spectroscopy. The refractive index and extinction coefficient as functions of the wavelength for the layers used in the solar cell are shown in Figs. 1(a) and 1(b), respectively.

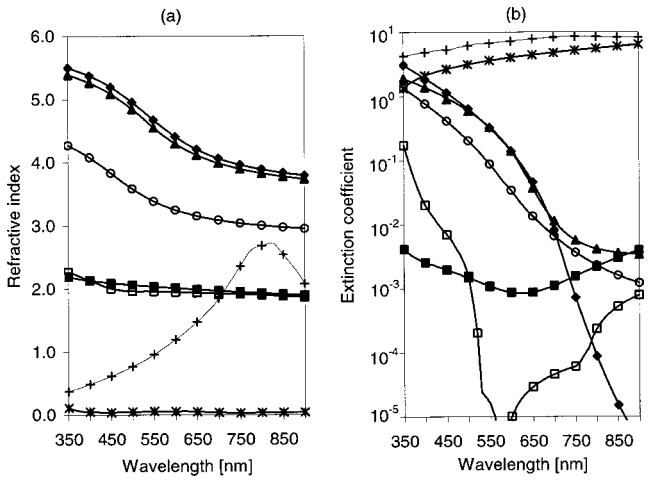


FIG. 1. The refractive index (a) and extinction coefficient (b) as function of the wavelength for the layers used in the simulated solar cell: (♦) intrinsic *a*-Si:H, (▲) *n*-type *a*-Si:H, (○) *p*-type *a*-SiC:H, (■) $SnO_2$:F, (□) ZnO, (*) Ag, + Al.

### B. Deposition and characterization of *a*-Si:H solar cells

Four single junction *a*-Si:H solar cells each with different thicknesses of the intrinsic layer were deposited on Asahi U-type substrate, which is textured $SnO_2$:F transparent conductive oxide (TCO) deposited on glass. The solar cells have the following structure: Asahi U-type/*p*-type *a*-SiC:H (9 nm)/ intrinsic *a*-Si:H (150–600 nm)/ *n*-type *a*-Si:H (20 nm)/ Ag (300 nm). The solar cells were characterized by illuminated $J-V$ measurements and by spectral response measurements. The external parameters of the solar cells determined from $J-V$ characteristics under AM1.5 standard illumination are presented in Table I.

## III. GENPRO2 OPTICAL PROGRAM

The GENPRO2 is a semiempirical optical program that calculates optical properties such as the total reflection, the total transmission, and the generation profile of a multilayer optical system with rough interfaces. The GENPRO2 program is based on the multirough-interface optical model.[14] The main assumption of the multirough-interface model is that it regards a rough interface as a flat interface with small disturbances that cause the scattering of light. This assumption means that a rough interface reflects and transmits the same amount of light as a flat interface and that for the calculation

TABLE I. The short-circuit current density $J_{sc}$, the open-circuit voltage $V_{oc}$, the fill factor, and the efficiency of the solar cells determined from $J-V$ characteristics under AM1.5 standard illumination. The cell area is 0.1 $cm^2$.

| *i*-layer thickness (nm) | $J_{sc}$ (mA $cm^{-2}$) | $V_{oc}$ (V) | Fill factor | Efficiency (%) |
|---|---|---|---|---|
| 150 | 12.54 | 0.79 | 0.69 | 6.89 |
| 300 | 14.96 | 0.82 | 0.71 | 8.79 |
| 450 | 16.56 | 0.82 | 0.69 | 9.40 |
| 600 | 16.71 | 0.79 | 0.71 | 9.48 |

of the reflectance and the transmittance of the interface an approach based on the theory of thin film optics using the Fresnel amplitude coefficients[15] can be used. This approach of using the Fresnel amplitude coefficients is in the multirough-interface model extended to multilayer optical systems, in which due to the scattering the individual layers are assumed to be incoherent.

Further the multirough-interface model assumes that the total reflected (transmitted) light at a rough interface is the sum of the specular and the diffuse fractions of the reflected (transmitted) light. The relation between the diffuse part of the reflected (transmitted) light and the total reflected (transmitted) light is as follows:

$$R_d(\lambda,\theta_{\text{in}},\theta_{\text{out}})=C_R(\lambda)f_R(\theta_{\text{in}})f_R(\theta_{\text{out}})R_0(\lambda), \tag{1}$$

$$T_d(\lambda,\theta_{\text{in}},\theta_{\text{out}})=C_T(\lambda)f_T(\theta_{\text{in}})f_T(\theta_{\text{out}})T_0(\lambda), \tag{2}$$

where $R_d$ ($T_d$) is the diffused reflectance (transmittance), $R_0$ ($T_0$) is the reflectance (transmittance) of a flat interface, $C_R$ ($C_T$) is the haze parameter for reflected (transmitted) light, $f_{R,T}(\theta_{\text{in}})$ describes the angle dependence of the incident light, and $f_{R,T}(\theta_{\text{out}})$ gives the angle dependence of the outgoing diffused light. The GENPRO2 program requires these descriptive scattering parameters of a rough interface as input. When knowing the haze parameter and the angular dependence of the diffuse light the GENPRO2 program calculates the contributions of the diffuse light to the generation in the individual layers of an optical system taking the enhanced optical path of the diffuse light into account. In general, the descriptive scattering parameters of a rough interface are obtained experimentally and therefore the GENPRO2 program is a semiempirical program.

## IV. CHARACTERIZATION OF THE ROUGH INTERFACE

A rough interface is described by the rms roughness and the scattering data, which include the haze parameter and the angular distribution of diffuse light. In this article we show that the descriptive scattering parameters that are used as input for the GENPRO2 program can be related to the interface rms roughness and we present the relevant relations.

Typical values of $\sigma_r$ of the TCO textured superstrates that are used in the fabrication of *a*-Si:H solar cells are in the range of 30–50 nm. The wavelength region of interest for single junction *a*-Si:H solar cells is between 400 and 800 nm. The wavelength that determines the amount of scattering is the effective wavelength in the medium from which the light reaches the rough interface. This effective wavelength is given by

$$\lambda_{\text{eff}}=\lambda_{\text{air}}/n_0(\lambda). \tag{3}$$

Here $n_0$ is the refractive index of the medium of incidence. In the wavelength region of interest, $\lambda_{\text{eff}}$ is for the TCO ($n_0\approx 2$) 200–400 nm and for the *a*-Si:H ($n_0\approx 4$) 100–200 nm. The $\lambda_{\text{eff}}$ in these media is comparable to or larger than the $\sigma_r$ of the interface between these media in *a*-Si:H solar cells. A modified scalar scattering theory that is explained in Sec. IV C can be applied to such rough surfaces to relate the specular reflectance of a rough interface to its $\sigma_r$.[16,17]

### A. Characterization of interface roughness in solar cells

The value of the rms roughness of the Asahi U-type substrate is found to be dependent on the scanned area measured with AFM and is higher for a larger scanned area. This area dependence indicates that a thickness variation is present in the substrate over distances larger than the range of a typical AFM scan of several micrometers. Transmission electron microscopy measurement on this TCO substrate revealed a thickness variation from 620 to 740 nm. Under the assumption that for light in the wavelength range of interest (300–900 nm) only a local roughness over an area less than 1 $\mu$m$^2$ is important we have used $\sigma_r=40$ nm in our simulations for the TCO/*p* interface. This value is an average from 20 measurements carried out on $3\times 3$ $\mu$m$^2$ scanned areas.

Deposition of a 9 nm *p*-type *a*-SiC:H did not result in an observable change of the surface roughness. Deposition of a 150 nm thick *a*-Si:H intrinsic layer resulted in a surface characterized by $\sigma_r=36$ and 300 nm thick layer resulted in a further reduction of the rms roughness to $\sigma_r=33$ nm. We assumed that the deposition of the 20 nm *n*-type *a*-Si:H layer on top of this did not further change the surface roughness significantly.

### B. Diffuse reflectance as a function of the rms roughness

For rough interfaces, which have $\sigma_r$ comparable to or smaller than $\lambda_{\text{eff}}$ of the medium of incidence, the scalar scattering theory can be applied to determine the specular reflectance of an interface. Bennett and Porteus[16] demonstrated that in the case of normal incidence the specular part of the total reflectance $R_s$ is related to $\sigma_r$ by

$$R_s=R_0\exp[-(4\pi\sigma_r n_0/\lambda)^2], \tag{4}$$

where $R_0$ is the reflectance of a flat surface. Under the assumption that the sum of the specular and the diffuse reflectance of a rough interface is equal to the reflectance of a perfectly smooth interface between the same materials ($R_s+R_d=R_0$) the diffuse reflectance using Eq. (4) becomes

$$R_d=R_0(1-\exp[-(4\pi\sigma_r n_0/\lambda)^2]). \tag{5}$$

Figures 2(a) and 2(b) present the ratio of $R_d$ to $R_0$ as calculated from Eq. (5) for light incident at a rough interface through Asahi U-type TCO and *n*-type *a*-Si:H, respectively, for several values of $\sigma_r$. It is important to note in Fig. 2(b) that the back contact interface acts as a nearly perfect diffuser for the reflected light in the wavelength range of interest when $\sigma_r$ is larger than 30 nm.

### C. Determination of diffuse transmittance

In a superstrate *a*-Si:H solar cell light enters the solar cell through the TCO layer. The TCO layer also introduces the first rough interface into a solar cell at which light is scattered. In order to investigate the scattering properties of the TCO rough surface we measured the total integrated transmission (TIT) of a simple optical system consisting of glass/medium/Asahi U-type substrate where the medium is either air or water. We noticed a substantial difference be-

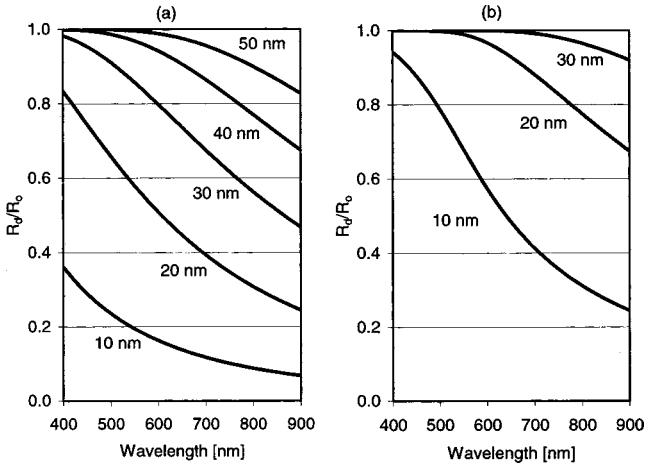


FIG. 2. The ratio of $R_d$ to $R_0$ as a function of wavelength for several values of the rms roughness of the rough interface: (a) Asahi U-type TCO material and (b) $n$-type $a$-Si:H.

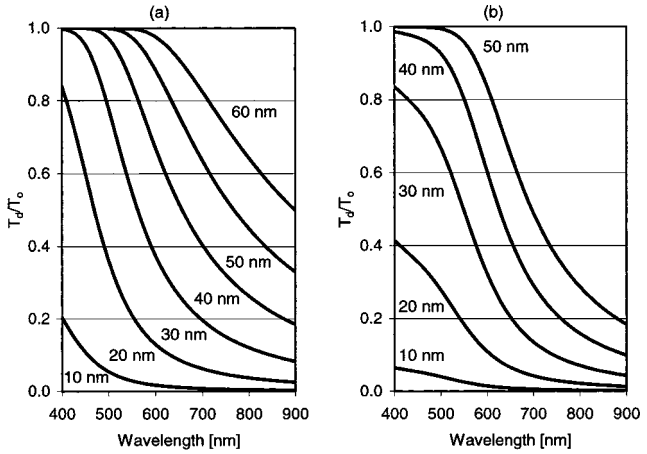


FIG. 4. The ratio of $T_d$ to $T_0$ as function of wavelength for several values of $\sigma_r$ for: (a) the TCO/$p$ interface and (b) the $p/i$ interface.

tween the measured TIT and the simulated results of this optical system in the short wavelength region assuming flat interfaces (see Fig. 3). This difference is caused by an enhanced absorption of light within the TCO layer due to the scattering at the rough interface.

We evaluated the scattering properties of the Asahi U-type TCO rough surface for transmitted light by comparing the measured TIT with the simulations, in which the interface between the medium and the TCO was rough. In the simulations we used Eq. (5) to calculate the diffuse reflectance at the rough TCO/medium interface with $\sigma_r = 40\,\text{nm}$. For the diffuse transmittance we first assumed a square dependence on $(\sigma_r/\lambda_{\text{eff}})$ similar to the case of diffuse reflectance and we used the following relationship:

$$T_d \cong T_0 \times (1-\exp[-(2\pi\sigma_r C_{\text{corr}}(n_0\cos\theta_0 - n_1\cos\theta_1)/\lambda_{\text{eff}})^2]). \tag{6}$$

Here $T_d$ is the diffuse transmittance, $T_0$ is the transmittance of a smooth interface between two media, which are characterized by refractive indices $n_0$ and $n_1$, $\theta_0$ is the angle of incidence, and $\theta_1$ is the angle of refraction of the specular beam. Notice that when $C_{\text{corr}}=1$, Eq. (6) reduces to the formula, which was derived by Carniglia.[18] Using the original formula as derived by Carniglia we could not obtain a good match between the measured and simulated TIT values. In order to obtain a good match, we introduced a correction factor $C_{\text{corr}}$. Even using the correction factor $C_{\text{corr}}$ in Eq. (6) no good match was obtained.

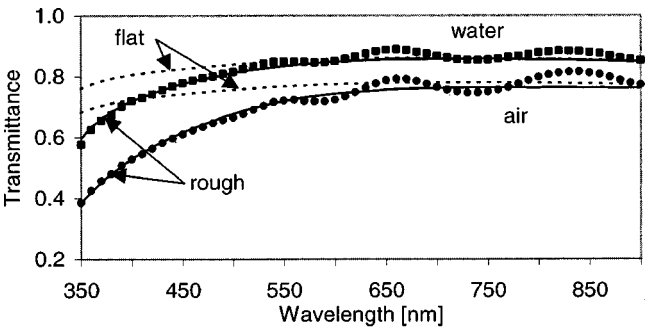


FIG. 3. The total integrated transmission as function of wavelength of glass/medium/Asahi U-type substrate optical system. The dots are the measured data [medium: (■) water (●) air], the full lines represent the fits of simulated total transmittance taking the rough interface into account, the dashed lines represent the total transmittance of the system with flat interfaces.

In order to extract the diffuse transmittance of the rough Asahi U-type TCO as a function of λ and $\sigma_r$ we assumed a function describing the diffuse transmittance of the following form:

$$T_d = T_0(1-\exp[-(C_1\sigma_r/\lambda)^{C_2}]), \tag{7}$$

where $C_1$ and $C_2$ are the fitting parameters. From the fitting procedure, in which we have matched the measurements of the TIT with the simulations, we extracted the following formula:

$$T_d = T_0(1-\exp[-(4\pi\sigma_r C\ |n_0-n_1|/\lambda)^3]). \tag{8}$$

In this formula $C$ is a factor that depends on the two media. Figure 3 shows the results of the measurements and simulations, in which Eq. (8) was used for calculating the diffuse transmittance, when air or water were used as the leveling medium. It is important to note that $\lambda/|n_0-n_1|$ is used as the effective wavelength instead of the effective wavelength as defined by Eq. (3). We noticed that when $|n_0-n_1|$ increases $C$ approaches 1.

In our simulations we used Eq. (8) to calculate the diffuse transmittance for all rough interfaces in the $a$-Si:H solar cell. Figure 4 shows the ratio of $T_d$ to $T_0$ for the TCO/$p$ and $p/i$ interfaces for $C=1$ and several values of $\sigma_r$ as calculated from Eq. (8).

## V. SIMULATIONS

### A. Simulations of external quantum efficiency

From spectral response measurements of the solar cell the absolute external quantum efficiency can be determined, which contains valuable information about the contributions of both electronic and optical properties of the solar cell materials to the photovoltaic performance. The absolute ex-

ternal quantum efficiency is defined as the number of charge carriers collected (from all layers of the device) per incident photon at each wavelength λ. This quantum efficiency is defined as

$$\mathrm{QE}(\lambda)=\sum_{\text{layers}} \mathrm{QE}_{\mathrm{op}}(\lambda)\,\eta_g(\lambda)\mathrm{QE}_{\mathrm{el}}(\lambda), \tag{9}$$

where $\mathrm{QE}_{\mathrm{op}}$ is the optical quantum efficiency, which is a measure for the probability of a photon being absorbed. The quantum efficiency for carrier generation $\eta_g$ represents the number of electron–hole pairs generated by one absorbed photon and can be assumed to be unity. The electrical quantum efficiency $\mathrm{QE}_{\mathrm{el}}$ reflects the probability that a photogenerated carrier is collected. When using the term ''quantum efficiency (QE)'' in this article we mean the above defined absolute external quantum efficiency.

By applying a sufficiently large reverse bias voltage during the spectral response measurement all photogenerated carriers are collected, which implies that $\mathrm{QE}_{\mathrm{el}}$ is unity. In that case the measured QE represents the optical quantum efficiency, which can be simulated using the GENPRO2 program. The output of GENPRO2 is the generation profile in the solar cell as a function of depth. Under the assumption that all photogenerated carriers are collected, the total generation calculated per incident photon in the intrinsic *a*-Si:H layer of the solar cell represents the experimental QE of the solar cell measured at a reverse bias.

In our simulations all rough interfaces in the solar cell (TCO/*p*, *p*/*i*, *i*/*n*, and *n*/Ag) can contribute to the scattering. The diffuse reflectance and transmittance, which are required input parameters for the GENPRO2 program, were calculated for all rough interfaces in *a*-Si:H solar cells using Eqs. (5) and (8), respectively, with $C=1$ in Eq. (8). Based on the AFM results we used the same $\sigma_r$ for the TCO/*p* and *p*/*i* interfaces, and the same value of $\sigma_r$ for the *i*/*n* and *n*/Ag interfaces. The angular distribution of the diffuse light was described by the $\cos^2$ function. For the back metal interface a uniform angular distribution of the diffuse light was used.

Using the experimentally determined values of $\sigma_r$ of the rough interfaces in the four fabricated *a*-Si:H solar cells and the above described approach to model the diffuse reflectance and transmittance, we calculated the QE for each of the four solar cells. We obtain a good agreement between the simulated QE and the QE measured at $-1$ V for all four cells as shown in Fig. 5. Because the optical model, which is implemented in the GENPRO2 program, is developed to simulate structures with *rough* interfaces, the optical interference is of minor importance. Therefore an incoherent simulation is carried out in order to keep the model simple. This incoherent simulation can, however, lead to small deviations in the QE characteristics for optical systems, in which there is a significant contribution of specular fraction of light.

In order to obtain good agreement between the simulated and the measured QE a buffer layer was inserted between the *n*-type *a*-Si:H layer and the Ag back contact in our simulated solar cell structure. This buffer layer is realized in the simulations by inserting a thin 1.5 nm layer having optical properties similar to Al, as proposed by Stiebig *et al.*[7] This

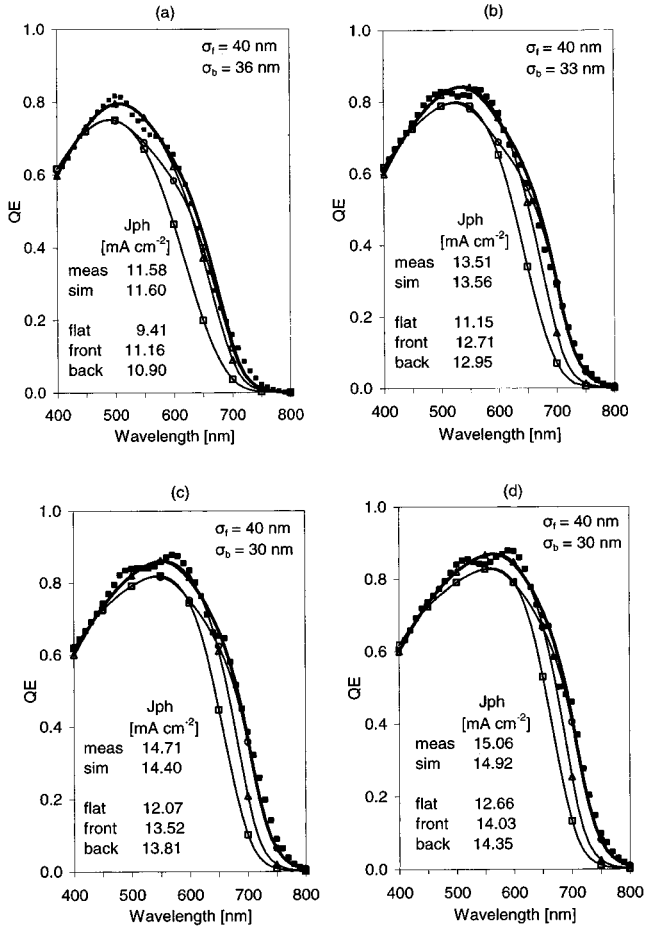


FIG. 5. The measured (■ points) and simulated (lines) QE of the four single junction *a*-Si:H solar cells each with a different thickness of the intrinsic layer: (a) 150 nm, (b) 300 nm, (c) 450 nm, and (d) 600 nm. The simulated QE curves: (i) all interfaces are flat (-□-), (ii) only the front interfaces (TCO/*p* and *p*/*i*) are rough (-△-), (iii) only the back interfaces (*i*/*n* and *n*/metal) are rough (-○-), and (iv) all interfaces are rough (full line). $\sigma_f$ ($\sigma_b$) is the rms roughness of the front (back) interfaces of the cell.

buffer layer accounts for the lower reflectivity of the practical Ag back contact, which may be due to intermixing of Ag with silicon.[19]

Figure 5 illustrates the effect of the front and back contact texture on the QE assuming that: (i) all interfaces are flat, (ii) only the front interfaces of the cell (TCO/*p* and *p*/*i*) are rough, (iii) only the back interfaces (*n*/metal and *i*/*n*) are rough, and (iv) all interfaces are rough. These simulations demonstrate the advantage of modeling, which enables us to investigate solar cell structures that are difficult to fabricate in practice or to evaluate the effect of particular model parameters separately. From the QE curves we calculated the photogenerated current density $J_{\mathrm{ph}}$ using the standard AM1.5 spectrum in the wavelength range from 400 to 900 nm. The values of the $J_{\mathrm{ph}}$ are also included in Fig. 5. The results clearly show that implementation of rough interfaces in *a*-Si:H solar cells leads to an enhanced absorption in the intrinsic layer. In the case of our superstrate solar cells the gain in $J_{\mathrm{ph}}$ is around $2.3\,\mathrm{mA\,cm^{-2}}$. This gain is only slightly dependent on the thickness of the intrinsic layer.

The simulation results of the QE reveal trends in the

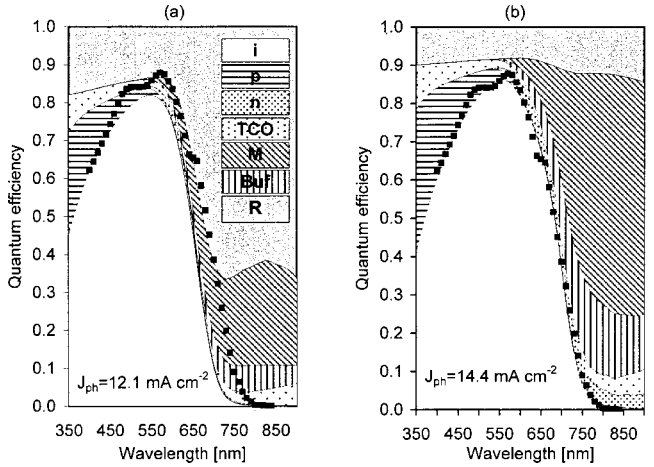


FIG. 6. The total reflection of an *a*-Si:H solar cell with a 1.5 nm thick buffer layer between the *n*-type *a*-Si:H and Ag and the absorption in the individual layers expressed in terms of QE: (a) solar cell with flat interfaces, and (b) solar cell with rough interfaces. The buffer layer has optical properties similar to Al. The dots are the measured QE data of the experimental cell with a 450 nm thick intrinsic layer. The photogenerated current density calculated from the simulated QE is included. The filled patterns correspond to: (*i*) intrinsic *a*-Si:H layer, (*p*) *p*-type *a*-SiC:H, (*n*) *n*-type *a*-Si:H layer, (TCO) TCO layer, (*B*) buffer layer, (*R*) total reflection.

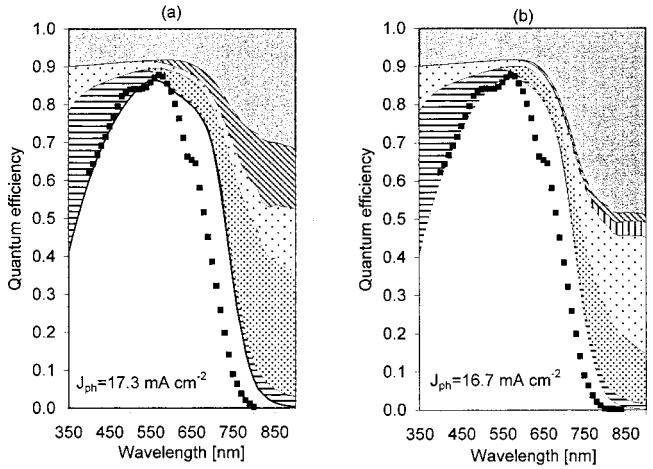


FIG. 7. The total reflection of an *a*-Si:H solar cell and the absorption in the individual layers expressed in terms of QE: (a) solar cell with an ideal Ag contact, (b) solar cell with a ZnO/Ag back contact. The dots are the measured QE data of the experimental cell. The patterns have the same meaning as in Fig. 6. The photogenerated current density calculated from the simulated QE is included.

optical behavior of *a*-Si:H solar cell when scattering is applied at various interfaces in the solar cell. It is illustrative to discuss the influence of scattering for two wavelength regions: the short wavelength region from 350 to 550 nm and the long wavelength region from 550 to 900 nm. The back contact roughness has no effect on the QE in the short wavelength region compared to solar cells with flat interfaces. Below $\lambda = 450$ nm scattering at the front rough interfaces causes a slight decrease in the QE while above $\lambda = 450$ nm this scattering contributes to a large absorption enhancement in the active layer of the cell. The major contribution of light scattering at the front interfaces to the QE is in the wavelength range between 450 and 650 nm. Above $\lambda = 650$ nm scattering at the back contact begins to play a dominant role in increasing the QE.

### B. Simulations of absorption in individual layers of *a*-Si:H *p-i-n* solar cell

The experimental QE is related to the absorption of light in the intrinsic *a*-Si:H layer and does not reveal the individual absorption losses in the other layers of the solar cell. We used the simulations to study the influence of the interface roughness on the absorption in all layers of the solar cell, which is very difficult to carry out experimentally. For comparison the total absorption in the individual layers and the total reflection of the solar cell is expressed in terms of the QE.

Figure 6 demonstrates trends in the optical behavior of a superstrate *a*-Si:H solar cell with a 450 nm thick intrinsic layer simulated with the above mentioned thin buffer layer, of which the optical properties are similar to Al. Figure 6(a) shows the results in the case where all interfaces in the cell are flat and Fig. 6(b) in the case where all interfaces are rough. In the latter case the $\sigma_r$ of the front contact interfaces is 40 nm and the $\sigma_r$ of the back contact interfaces is equal to 30 nm. These values of $\sigma_r$ are determined from the AFM measurements on the actual superstrate and the experimental solar cell. We note that scattering at the front rough interfaces causes a decrease in the QE below $\lambda = 450$ nm due to a stronger absorption in the TCO and *p* layer. Scattering at the back contact of the cell increases the QE in the long wavelength region but also causes an increased absorption in the *n* layer and metal. The major loss in the long wavelength region due to scattering is the absorption in the metal contact layer including the thin buffer layer. This cell is difficult to optimize because any improvement of the *n* layer or the TCO leads to a negligible enhancement of the QE in the long wavelength region. Therefore, a further enhancement of light absorption in the intrinsic layer can be expected from increasing the reflectivity of the back metal contact.

We have simulated a solar cell with an *ideal* Ag contact, which means that there is no intermixing between the *n*-type *a*-Si:H layer and the Ag. We also investigated the effect of introducing a ZnO layer between the *n*-type *a*-Si:H layer and Ag. The type of the back contact strongly influences the absorption in the individual layers of the cell. The results for a 450 nm thick superstrate solar cell with an ideal Ag back contact or a ZnO/Ag back contact are shown in Fig. 7 using the experimental values of $\sigma_r$.

The difference in the $J_{ph}$ between the cell with the thin Al buffer layer and an ideal Ag contact is not large when the interfaces are flat: $12.1\,\mathrm{mA\,cm^{-2}}$ compared to $12.4\,\mathrm{mA\,cm^{-2}}$, respectively. When rough interfaces are introduced in the cell with a textured superstrate, the difference between the $J_{ph}$ increases to $2.9\,\mathrm{mA\,cm^{-2}}$ [see Figs. 6(b) and 7(a)]. In the case of an ideal Ag back contact the loss due to the absorption in the nonactive layers is distributed among the *n* layer, TCO, and metal. Therefore a further improvement in the QE of this cell can be expected by optimizing the quality and the thickness of the *n* layer and/or the TCO. In practice, a high reflectivity at the back contact is achieved by

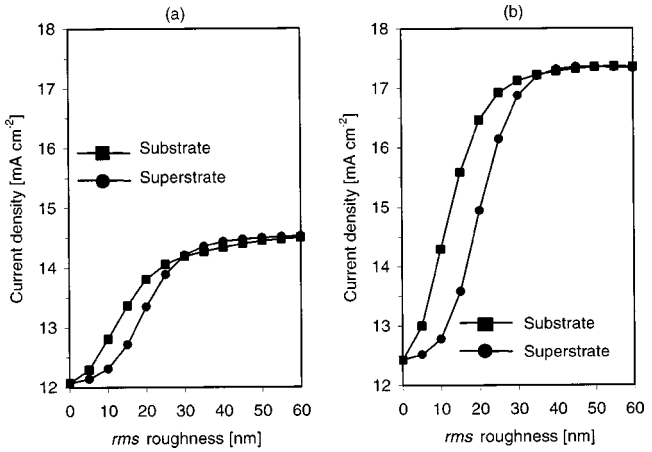


FIG. 8. The gain in the photocurrent density as a function of the carrier electrode roughness calculated from the QE of the solar cell: (a) solar cell with a thin Al buffer layer at the back contact, (b) solar cell with an ideal Ag back contact.

introducing a TCO layer between the *n* layer and Ag contact. In the case where a ZnO/Ag back contact is applied the $J_{ph}$ is not as high as in the case of an ideal Ag back contact. Nevertheless, it is 2.3 mA cm$^{-2}$ higher, when compared to a cell with a thin Al buffer layer [see Figs. 6(b) and 7(b)]. The simulations show that the QE hardly changes when the thickness of the ZnO layer is varied between 50 and 300 nm, as is observed experimentally.[20] The change in the $J_{ph}$ is less than 0.5%. However, reducing the thickness of the *n*-type layer to 5 nm in the solar cell structure with a 100 nm ZnO layer at the back contact results in a $J_{ph}$ of 17.3 mA cm$^{-2}$, compared to 16.7 mA cm$^{-2}$ for a 20 nm thick *n*-type layer. This represents an increase of more than 3%. Notice that the value of 17.3 mA cm$^{-2}$ for the $J_{ph}$ obtained by reducing the *n*-type layer thickness is fortuitously the same as when using an ideal Ag back contact.

### C. Effect of carrier electrode roughness

Deposition of *a*-Si:H on a textured substrate smoothens the rough surface. In the superstrate configuration, we observed a decrease of around 10 nm in the $\sigma_r$ after deposition of 450 nm thick *a*-Si:H film. We expect that in a substrate type *a*-Si:H cell the roughness of the front contact interface is similarly influenced by the deposition of the intrinsic layer. We have simulated the effect of increasing roughness of the the carrier electrode on the gain in photogenerated current density for both superstrate and substrate *a*-Si:H solar cells. In the simulations we assume that when increasing the rms roughness of the carrier electrode up to 10 nm, the other contact electrode is flat. Above 10 nm the rms roughness of the carrier electrode is 10 nm higher than the other contact interface. Figures 8(a) and 8(b) show the results for a solar cell with a thin Al buffer layer and an ideal Ag contact, respectively. The results demonstrate that increasing the rms roughness from $\sigma_r = 0$ to $\sigma_r = 35$ nm leads to a higher gain in the $J_{ph}$ in the substrate type solar cell compared to the superstrate type cell, while for $\sigma_r > 35$ nm the superstrate cell shows a slightly higher gain in the $J_{ph}$. For $\sigma_r > 60$ nm, the $J_{ph}$ saturates for both superstrate and substrate type solar cell. The $J_{ph}$ of the solar cell with the thin Al buffer layer saturates at 14.55 mA cm$^{-2}$. The current density of the cell with the ideal Ag contact reaches its highest value of 17.35 mA cm$^{-2}$ for $\sigma_r$ of around 50 nm for the carrier electrode. The results point out that for $\sigma_r < 35$ nm scattering at the back contact of the solar cell is more efficient in enhancing the absorption in the intrinsic layer than scattering at the front contact. When the intrinsic layer is thinner the difference between the rms roughnesses of the contact interfaces becomes smaller and that narrows the difference in gain in the $J_{ph}$ between the superstrate and substrate solar cells.

## VI. CONCLUSIONS

Using computer modeling we investigated the effect of back contact and interface roughness on the optical properties of *a*-Si:H solar cells by varying the rms roughness of the textured interfaces. The relations between the input parameters, which describe the diffuse part of reflected and transmitted light at a rough interface, and $\sigma_r$ of the interface are presented. By matching the measurements of the total integrated transmission we extracted the diffuse transmittance of the rough Asahi U-type/air interface. The diffuse transmittance is exponentially dependent on the third power of the ratio of $\sigma_r$ and $\lambda$, as described by Eq. (8).

The $\sigma_r$ of the Asahi U-type substrate surface is experimentally determined to be 40 nm. Deposition of a 9 nm thick *p*-type *a*-SiC:H layer on the substrate does not change the surface roughness significantly. The $\sigma_r$ of the back interface is found to be dependent on the intrinsic layer thickness and decreases by about 2.5 nm per 100 nm of the intrinsic layer. Due to the high refractive index of *n*-type *a*-Si:H the back contact interface acts as a nearly perfect diffuser for the reflected light when $\sigma_r$ is above 30 nm.

In the short wavelength region (below 550 nm) the back contact roughness has almost no effect on the QE. Scattering at the front rough interfaces causes a decrease in the QE below 450 nm due to stronger absorption in the TCO and *p* layer. Above 450 nm scattering at the front rough interfaces contributes to a large beneficial absorption enhancement. The major contribution to the QE from light scattered at the front interfaces is in the wavelength range between 450 and 650 nm. Above 650 nm scattering at the back contact plays a dominant role in the improvement of the QE. Therefore, texture is needed at both front and back interfaces in order to achieve enhanced absorption in the complete wavelength spectrum.

The choice of the back contact strongly influences the QE and the absorption in the nonactive layers of the solar cell for wavelengths above 650 nm. The practical Ag back contact can be successfully simulated by introducing a thin buffer layer between the *n*-type *a*-Si:H and Ag back contact, which has optical properties similar to Al. The QE of the cell can be improved by using a ZnO buffer layer between the *n*-type *a*-Si:H and the Ag. Using a ZnO layer, the gain in the photogenerated current density due to scattering at rough interfaces in the solar cell is 4.2 mA cm$^{-2}$. In the case of an ideal Ag back contact the gain in the photogenerated current density can amount to almost 5 mA cm$^{-2}$ compared to a so-

lar cell with flat interfaces. Optimizing the quality and the thickness of the *n*-type layer and the TCO front electrode can further improve these values.

Increasing $\sigma_r$ of the carrier electrode from 0 to 35 nm leads to a higher gain in the photogenerated current density in a substrate type solar cell compared to a superstrate type cell, while for $\sigma_r > 35$ nm the superstrate cell shows a slightly higher gain in the photogenerated current density. Increasing the roughness of the carrier electrode above 35 nm leads to only a small gain in the photogenerated current density. For $\sigma_r > 60$ nm the photogenerated current density saturates for both superstrate and substrate solar cells.

## ACKNOWLEDGMENTS

The authors would like to acknowledge financial support from the Netherlands Agency for Energy and the Environment (NOVEM) and Akzo Nobel for this research work. The authors also like to thank Akzo Nobel Chemicals Research Center Arnhem for their assistance in carrying out the optical characterizations and Marc Zuiddam from DIMES for the AFM measurements.

[1] N. Höhne, R. Carius, and H. Wagner, Mater. Res. Soc. Symp. Proc. **507**, 107 (1998).
[2] H. Schade and Z. E. Smith, J. Appl. Phys. **57**, 568 (1985).
[3] J. Morris, R. R. Arya, J. G. O'Dowd, and S. Wiedeman, J. Appl. Phys. **67**, 1079 (1990).
[4] G. Tao, M. Zeman, and J. W. Metselaar, Sol. Energy Mater. Sol. Cells **34**, 359 (1994).
[5] T. Sawada, N. Terada, T. Takahama, H. Tarui, M. Tanaka, S. Tsuda, and S. Nakano, Sol. Energy Mater. Sol. Cells **34**, 367 (1994).
[6] F. Leblanc, J. Perrin, and J. Schmitt, J. Appl. Phys. **75**, 1074 (1994).
[7] H. Stiebig, A. Kreisel, K. Winz, N. Schultz, C. Beneking, Th. Eickhoff, and H. Wagner, in Proceedings of the 1st World Conference on Photovoltaic Energy Conversion, 1994, pp. 603–606.
[8] Y. Hishikawa, H. Tarui, and S. Kiyama, in Technical Digest of the 11th International Photovoltaic Science and Engineering Conference, 1999, pp. 219–220.
[9] J. Daey Ouwens, M. Zeman, J. Löffler, and R. E. I. Schropp, Proceedings of the 16th European Photovoltaic Solar Energy Conference and Exhibition, 2000 (to be published).
[10] J. Springer, A. Poruba, A. Fejfar, M. Vanecek, L. Feitknecht, N. Wyrsch, J. Meier, and A. Shah, Proceedings of the 16th European Photovoltaic Solar Energy Conference and Exhibition, 2000 (to be published).
[11] H. Schade and Z. E. Smith, Appl. Opt. **24**, 3221 (1985).
[12] G. Tao, PhD thesis, Delft University of Technology, The Netherlands, 1994.
[13] J. Wallinga, PhD thesis, University Utrecht, The Netherlands, 1998.
[14] R. E. I. Schropp and M. Zeman, *Amorphous and Microcrystalline Solar Cells: Modeling, Materials, and Device Technology* (Kluwer Academic, Dordrecht, 1998).
[15] J. M. Bennett and H. M. Bennett, *Handbook of Optics* (McGraw-Hill, New York, 1978).
[16] H. E. Bennett and J. O. Porteus, J. Opt. Soc. Am. **51**, 123 (1961).
[17] J. O. Porteus, J. Opt. Soc. Am. **53**, 1394 (1963).
[18] C. K. Carniglia, Opt. Eng. (Bellingham) **18**, 104 (1978).
[19] S. Guha, Optoelectron., Devices Technol. **5**, 201 (1990).
[20] S. S. Hegedus, W. A. Buchanan, and E. Eser, Conference Record of the 26st IEEE Photovoltaic Specialists Conference, 1997, pp. 603–606.